PRESSURE-IMPULSE DIAGRAM OF THE FLNG TANKS UNDER SLOSHING LOADS

S E Lee, The Korea Ship and Offshore Research Institute (Lloyd's Register Foundation Research Centre of Excellence) at Pusan National University, Korea and Southampton Marine and Maritime Institute, University of Southampton, UK, **J K Paik**, Pusan National University, Korea and University College London, UK.

SUMMARY

Sloshing impact loads can cause severe structural damage to cargo tanks in liquefied natural gas floating production storage offloading units (LNG-FPSOs or FLNGs). Studies of sloshing can be classified into two types, namely, hydrodynamics-related and structural mechanics-related studies. This study is a sequel to the authors' previous studies (Paik et al. 2015; Lee et al. 2015), but is more related to issues of structural mechanics. In this study, a new method for probabilistic sloshing assessment, which has been previously developed by the authors, is briefly explained. The nonlinear impact structural response characteristics under sloshing impact loads are examined by a nonlinear finite element ANSYS/LS-DYNA method. An iso-damage curve, representing a pressure-impulse diagram, is derived for the self-supporting prismatic-shape IMO B type LNG cargo containment system of a hypothetical FLNG. The insights developed from this work can be useful for the damage-tolerant design of cargo tanks in FLNGs.

NOMENCLATURE

C	Cowper-Symonds coefficient
D	Maximum deformation level (mm)
I_a	Impulsive asymptote (bar·s)
I_o	Impulse (bar·s)
K	Spring stiffness (N/mm)
T	Natural period (s)
P_a	Quasi-static asymptote (bar)
P_o	Peak pressure (bar)
q	Cowper-Symonds coefficient
t_{dec}	Decay time of an impact action (ms)
t_{dur}	Duration time of an impact action (ms)
t_{dur}'	Idealized duration time of an impact action (ms)
t_o	Rise time of an impact action (ms)
x_{max}	Maximum dynamic displacement (mm)
α, β	Constants
$\dot{\varepsilon}$	Strain rate (mm/s)
ε_f	Fracture strain under a static load (mm)
ε_{fd}	Fracture strain under a dynamic load (mm)
ν	Poisson's ratio
ρ	Density of a material (kg/m^3)
σ_Y	Yield stress under a static load (N/mm^2)
σ_{Yd}	Yield stress under a dynamic load (N/mm^2)
ω	Natural circular frequency (rad/s)

1.   INTRODUCTION

Tank sloshing is unavoidable in a liquefied natural gas floating production storage offloading unit (LNG-FPSO or FLNG), due to the continuous loading and unloading processes, together with the effects of winds, waves and currents (Paik and Thayamballi, 2003, 2007). In many cases, repetitive sloshing impact loads can cause severe structural damage to LNG cargo containment systems (CCS) and their sub-structures.

Studies of sloshing can be classified into two kinds: hydrodynamics-related studies that aim to identify the impact pressure profile over time, and structural mechanics-related studies that aim to calculate the dynamic structural damage. To quantify structural damage under sloshing impact loads, a number of extensive studies have been conducted over the last 50 years.

Classification societies, shipyards and third-party authorities have proposed their own assessment procedures (ABS 2006; DNV GL 2006; LR 2009; BV 2011; Hwang *et al* 2014; Ito *et al*. 2008; Nam *et al*. 2006; Pastool *et al*. 2005; Graczyk *et al*. 2007; Graczyk and Moan 2008; Kuo *et al*. 2009). In recent years, numerical and experimental studies on loads and strength of sloshing impacts have also been undertaken in the literature (Paik and Shin 2006; Nasar *et al*. 2008; Hirdaris *et al*. 2010; Brizzolara *et al*. 2011; Zhao *et al*. 2013; Jiang *et al*. 2015; Kim *et al*. 2017; Liu *et al*. 2017; Xu *et al*. 2017; Zhang *et al*. 2017).

It has been widely recognised, however, that the sloshing impact loads obtained from current procedures might not represent the entire set of credible sloshing scenarios, as these procedures have been conducted for specific environmental conditions or for limited ranges of tank resonant periods.

To improve the sloshing scenario sampling, the authors have previously proposed a fully probabilistic design procedure that provides guidelines to be followed in all the tasks involved, from selecting credible scenarios probabilistically to determining the design sloshing loads (Paik *et al*. 2015), and conducting the nonlinear dynamic structural analysis under sloshing loads (Lee *et al*. 2015). As a sequel to that design procedure, this study applies a new approach as shown in Figure. 1 that utilises a pressure-impulse (P-I) diagram for assessing the extent of damage to the cargo tanks in FLNG units.
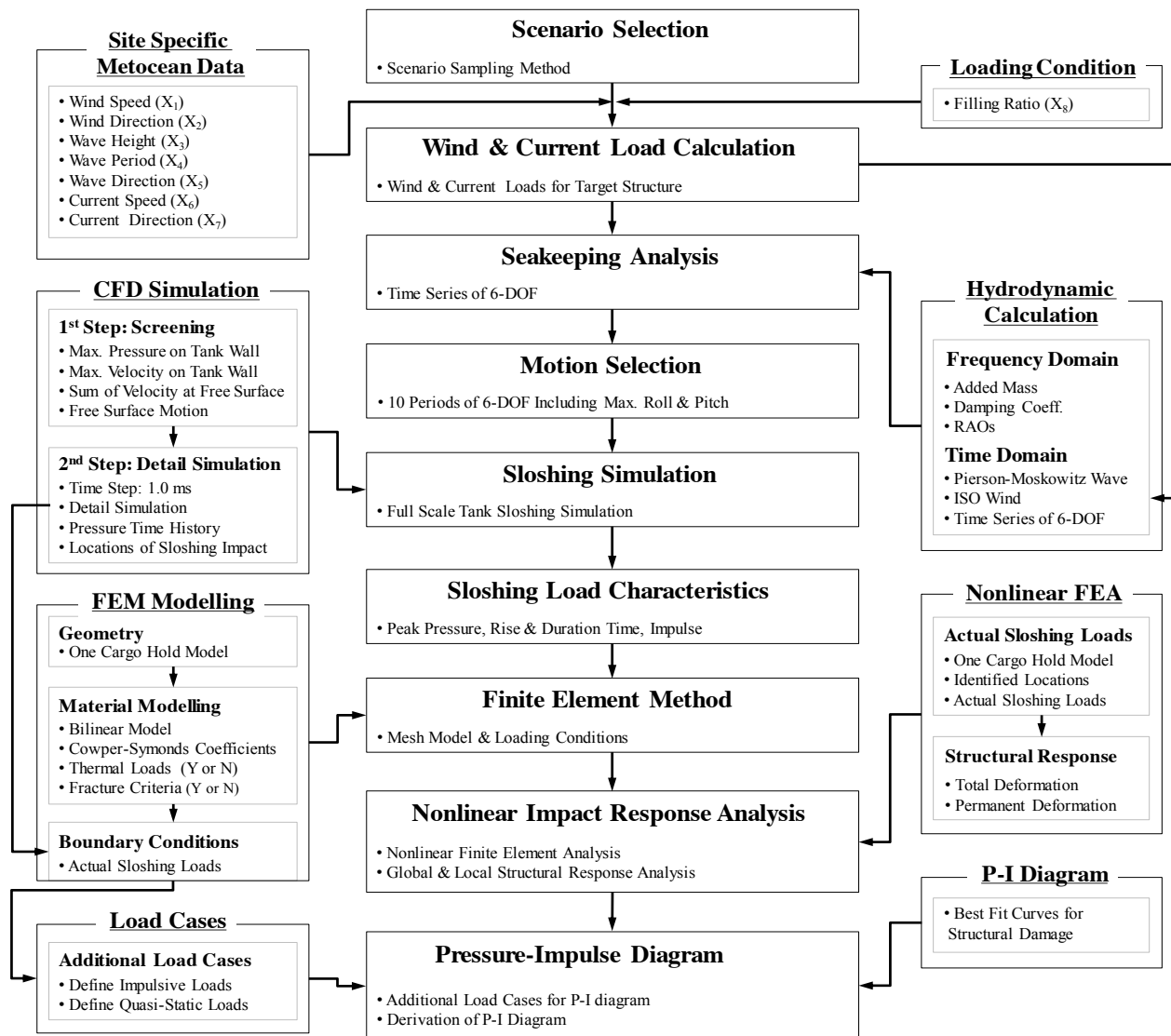
Figure 1 flowchart

Site Specific Metocean Data
- Wind Speed (X_1)
- Wind Direction (X_2)
- Wave Height (X_3)
- Wave Period (X_4)
- Wave Direction (X_5)
- Current Speed (X_6)
- Current Direction (X_7)

CFD Simulation

1st Step: Screening
- Max. Pressure on Tank Wall
- Max. Velocity on Tank Wall
- Sum of Velocity at Free Surface
- Free Surface Motion

2nd Step: Detail Simulation
- Time Step: 1.0 ms
- Detail Simulation
- Pressure Time History
- Locations of Sloshing Impact

FEM Modelling

Geometry
- One Cargo Hold Model

Material Modelling
- Bilinear Model
- Cowper-Symonds Coefficients
- Thermal Loads (Y or N)
- Fracture Criteria (Y or N)

Boundary Conditions
- Actual Sloshing Loads

Load Cases

Additional Load Cases
- Define Impulsive Loads
- Define Quasi-Static Loads

Scenario Selection
- Scenario Sampling Method

Wind & Current Load Calculation
- Wind & Current Loads for Target Structure

Seakeeping Analysis
- Time Series of 6-DOF

Motion Selection
- 10 Periods of 6-DOF Including Max. Roll & Pitch

Sloshing Simulation
- Full Scale Tank Sloshing Simulation

Sloshing Load Characteristics
- Peak Pressure, Rise & Duration Time, Impulse

Finite Element Method
- Mesh Model & Loading Conditions

Nonlinear Impact Response Analysis
- Nonlinear Finite Element Analysis
- Global & Local Structural Response Analysis

Pressure-Impulse Diagram
- Additional Load Cases for P-I diagram
- Derivation of P-I Diagram

Loading Condition
- Filling Ratio (X_8)

Hydrodynamic Calculation

Frequency Domain
- Added Mass
- Damping Coeff.
- RAOs

Time Domain
- Pierson-Moskowitz Wave
- ISO Wind
- Time Series of 6-DOF

Nonlinear FEA

Actual Sloshing Loads
- One Cargo Hold Model
- Identified Locations
- Actual Sloshing Loads

Structural Response
- Total Deformation
- Permanent Deformation

P-I Diagram
- Best Fit Curves for Structural Damage

Figure 1: Procedure of a probabilistic design approach to assessing structural damage under sloshing impact loads.

In general, the P-I diagram is a useful design tool that structural design engineers are able to easily assess the response to applied loads. With defined damage level, the diagram indicates the combinations of load and impulse that will cause a specific damage level. In the early days, the P-I diagram method has most commonly been used for assessing animal and human injuries or for analysing structural damage from blast loads (Jarrete 1968; Smith and Hetherington 1994; Baker *et al.* 1983; Mays and Smith 1995; Merrifield 1993; Li and Meng 2002a, 2002b; Fallah and Louca 2007; Ma *et al.* 2007; Parlin *et al.* 2014; Lan and Crawfird 2003; Scheider 1998; Wesevich and Oswald 2005; Shi *et al.* 2008; Sohn *et al.* 2013). This method involves applying a single degree of freedom (SDOF) model (Li and Meng 2002b; Fallah and Louca 2007; Ma *et al.* 2007; Parlin *et al.* 2014; Lan and Crawfird 2003; Scheider 1998) and a finite element method (FEM) (Lan and Crawfird 2003; Scheider 1998; Wesevich and Oswald 2005; Shi *et al.* 2008; Sohn *et al.* 2013). In this study, the authors examine the feasibility of using the P-I method to

quantify structural damage to cargo tanks in FLNG units as shown in Figure. 2.
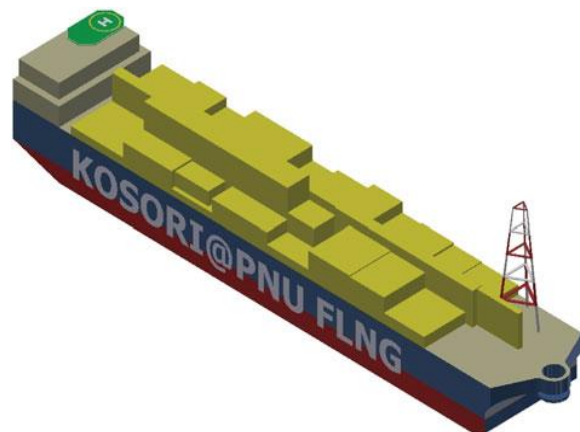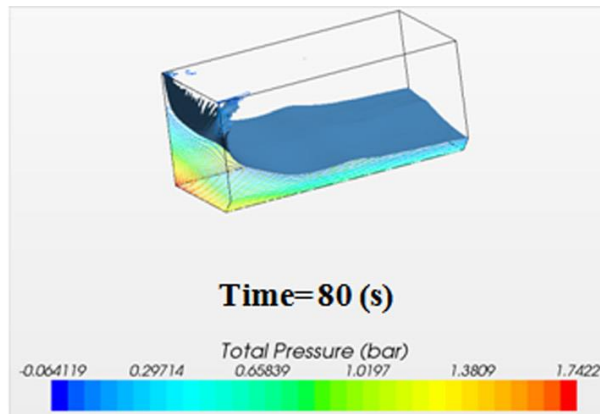
Figure 2: A hypothetical FLNG (Lee *et al.* 2015).

Figure 3: An example of the pressure distribution inside the LNG tank (Paik *et al*. 2015)
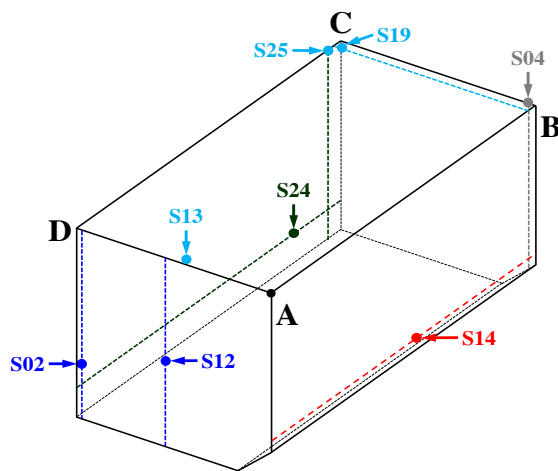

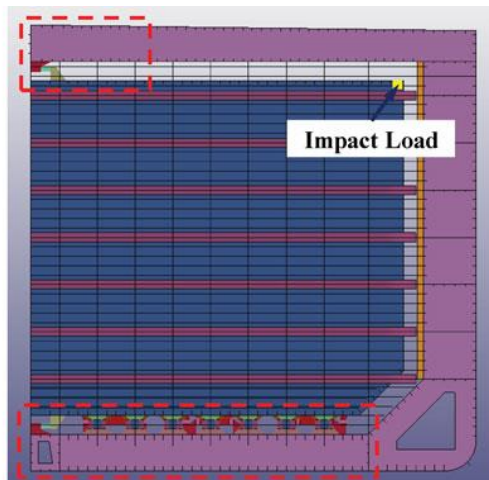Figure 4: identified sloshing impact locations from 30 credible scenarios (Lee *et al*. 2015)

Figure 5: An example of the FE model and the boundary conditions (Lee et al. 2015)

2.   PROBABILISTIC PROCEDURE OF SLOSHING ASSESSMENT

This chapter briefly summarises the developed probabilistic procedure of sloshing assessment. It can be outlined as follows:

Step 1
- Selecting credible sloshing scenarios through a probabilistic sampling method
- Finite volume method (FVM) mesh modelling for the wind and current loads
- Estimating the wind and current loads for all directions by computational fluid dynamics (CFD)
- Seakeeping analysis in the frequency- and time-domains taking into account the wind, wave, and current loads
- Selecting a range of motion for sloshing simulations
- FVM mesh modelling of tank sloshing in full scale
- Performing sloshing CFD simulation (Figure. 3)
- Analysing the sloshing load characteristics for peak pressure, impulse and rise time
- Identifying locations of the sloshing impact (Figure. 4)

Step 2
- FEM mesh modelling
- Defining material modelling and boundary conditions (Figure. 5)
- Analysing a series of nonlinear structural responses under parametric sloshing loads
- Identifying the weakest location in a tank

Step 3
- Identifying the range of actual sloshing impact profiles from the CFD simulations
- Nonlinear FEM (NLFEM) series analyses for the weakest location
- Quantifying the extent of damage
- Deriving the P-I diagram of maximum deformation
- Estimating the impulsive and quasi-static asymptotes
- Evaluating the unit's structural capacity and safety

3.   CHARACTERISTICS OF THE P-I DIAGRAM

For structural designers, the primary objective for assessing the loading capacity of a target structure can be either to determine the maximum deflection or to assess the stress level at the end of the loading state. However, in the structural design of a dynamic system, the time history of the dynamic responses is also very significant. For practical design purposes, structural behaviour in response to an impact-pressure event can be conceptualised within three domains, depending on the ratio between the duration of an impact event, and the natural period of the structure. This evaluation is conducted as follows (NORSOK 2009):

- Quasi-static domain: $t_{dur}/T \geq 3$
- Dynamic domain: $0.3 \leq t_{dur}/T < 3$
- Impulsive domain: $t_{dur}/T \leq 0.3$

By plotting known responses, the spectra of maximum peak responses to the abovementioned three domains can

be illustrated, and the structural behaviour under a given loading can be clarified, as shown in Figure. 6. There are various forms of response spectra plots that can describe the relationships between the maximum value of a response parameter and characteristics of the dynamic system. Among these forms, the P-I diagram is widely used to represent the response spectrum for structural damage assessment, as illustrated in Figure. 7.
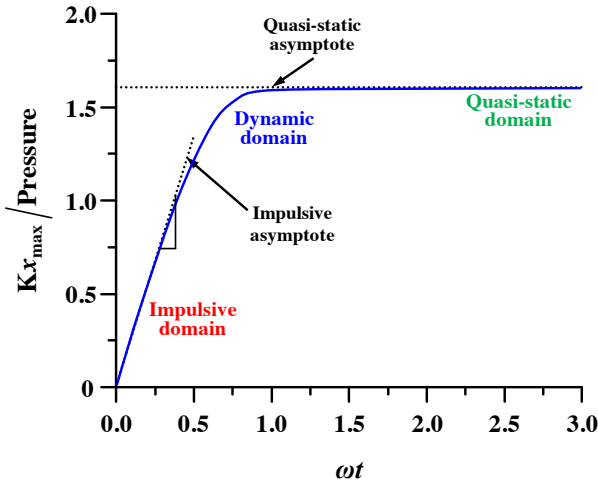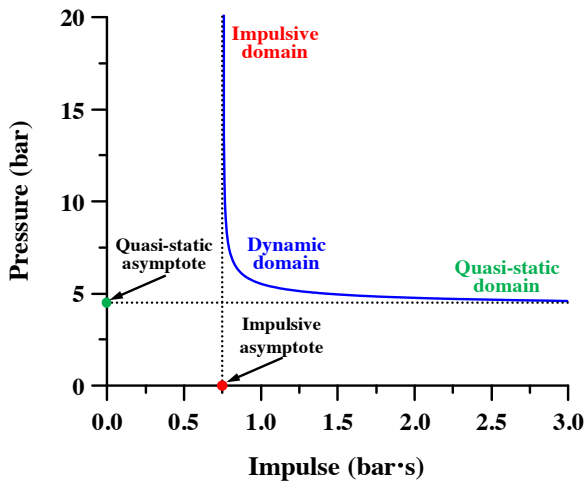

Figure 6: Typical response spectrum.

Figure 7: Typical pressure-impulse diagram.

Unlike the typical response spectrum plot, the P-I diagram allows a simple differentiation between behaviour domains, in the form of impulsive and quasi-static asymptotes. For estimating the structural safety of a dynamic system under combined pressure-impulse forces, plots in the diagram's left area and below a basis level indicate no specified damage, but plots in the right area and above the basis level indicate damage in excess of that level.

As shown in Figure. 8, if the dynamic system shows multiple plots of damage-level events in the P-I diagram, then each of these events represents damage, which may range from negligible to extreme, according to the damage criteria. In this regard, the P-I diagram method can serve as an efficient approach to quantifying structural damage levels, and this method can help structural engineers to systematically identify the safety limits and the structural capacity of a unit in response to expected impact pressure events.

4. FINITE ELEMENT MODELLING

4.1 GEOMETRY

A hypothetical barge-type FLNG with a Self-supporting, Prismatic-shape IMO type B (SPB) tank was developed, as shown in Figure. 5. This target structure has the following dimensions: length 411 m, breadth 80 m, depth 40 m, draft 15.1 m and total capacity 628 K. The details of the tank arrangement and a schematic drawing of a mid-ship section were presented in the authors' previous study (Paik *et al*. 2015).

4.2 MATERIAL MODEL

In the dynamic structural response analysis using the NLFEM, material properties are the major factors of concern, as yield stress and fracture strain vary along with the dynamic effects, and specifically the strain rate effects. The Cowper–Symonds model is usually applied to evaluate strain rate effects (Jones 1970; Paik 2003).

$$\frac{\sigma_{Yd}}{\sigma_Y} = 1.0 + \left(\frac{\dot{\varepsilon}}{C}\right)^{1/q} \tag{1}$$

$$\frac{\varepsilon_{fd}}{\varepsilon_f} = \left[1.0 + \left(\frac{\dot{\varepsilon}}{C}\right)^{1/q}\right]^{-1} \tag{2}$$

where σ_Y and ε_f are the yield stress and the fracture strain under static load; σ_{Yd} and ε_{fd} are the yield stress and the fracture strain under dynamic load; $\dot{\varepsilon}$ is the strain rate; and C and q is the experimentally determined Cowper-Symonds coefficients. MAT_PIECEWISE_LINEAR_PLASTICITY in ANSYS /LS-DYNA is adopted to take the elasto-plastic behaviour and strain rate into account. This analysis characterises not only the nonlinear stress-strain relationships of the material, but also the yield stress with factors *C* and *q* (ANSYS/LS-DYNA 2014).
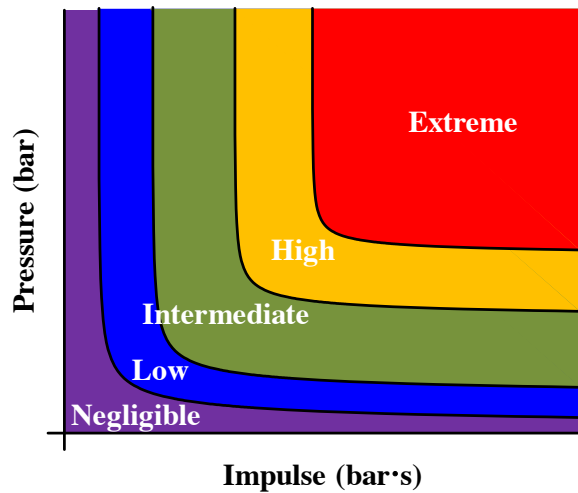
Figure 8: Damage level of P-I diagram.

The materials composing the tank and hull structures are aluminum and mild steel, respectively. The SPB tank and its supporting structures are assumed to be constructed of aluminum alloy at a temperature of -163°C, and the hull structures are of mild steel constructed at room temperature. The effects of thermal loads within the cargo tanks are not considered because this study is focused on the dynamic structural behaviour. The applied material properties obtained by the material coupon test are shown in Table 1. The insulation system is not included in this study.

Table 1: Material properties of cargo tanks

Units	Al. at -163°C	Mild steel at RT
ρ	2700	7889
ν	0.33	0.3
σ_Y	133.25	235.0
C	6500	40.4
q	4	5

4.3   LOADING AND BOUNDARY CONDITIONS

Characterising the sloshing impact load is one of the most challenging tasks in determining structural requirements. The actual sloshing loads can be conceptualised as impulsive loading, and characterised by the peak pressure, impulse and rise time, as shown in Figure. 9. In the parametric analyses, each sloshing load is conceptualised, and the results in terms of its ideal duration time, t_{dur}' are summarised in Table 2.

To simplify the NLFEM computations, the boundary conditions are set as symmetrical around the centre plane, and fixed at both ends of the hull structure, as explained in the authors' previous study (Lee *et al*. 2015). The total simulation time is set as three times the duration of an applied sloshing load, as a means to consider the dynamic stress propagation in the structural model.

Table 2: Actual sloshing load profiles

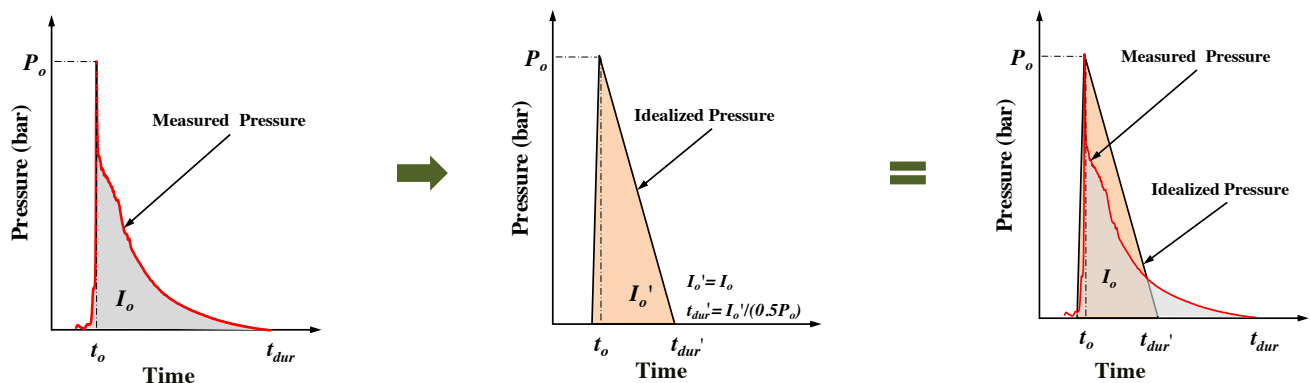| No.	t_o	P_o	t_{dec}	I_o	t_{dur}'
Scenario-02	18	15.31	292	0.95	124
Scenario-04	10	1.32	195	0.06	88
Scenario-12	67	7.45	1,388	1.33	356
Scenario-13	18	3.22	269	0.17	108
Scenario-14	35	0.71	643	0.10	279
Scenario-19	27	5.36	578	0.93	345
Scenario-24	22	0.59	769	0.09	316
Scenario-25	34	8.58	966	1.50	350

Figure 9: Idealisation of measured sloshing impact pressure characteristics applied in the dynamic structural analysis.
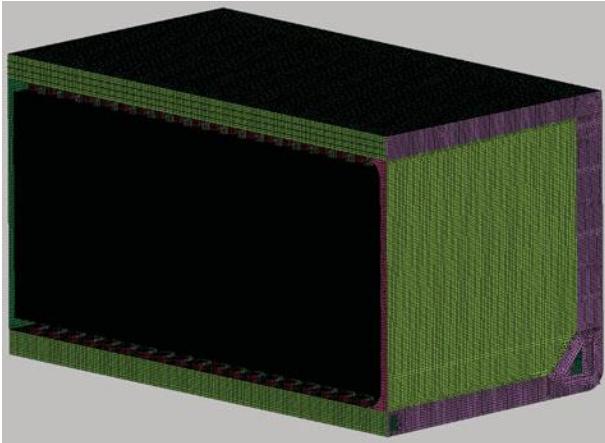
Figure 10: An example of the generated mesh model (Lee *et al*. 2015).

Table 3: Calculated impulse for parametric studies

P_o	t_{dur}'				
	88	108	124	316	350
0.592	0.026	0.032	0.037	0.094	0.103
1.324	0.058	0.071	0.082	0.209	0.231
3.225	0.142	0.174	0.199	0.510	0.564
5.361	0.236	0.289	0.331	0.847	0.926
8.587	0.378	0.463	0.530	1.357	1.502
15.312	0.674	0.825	0.946	2.420	2.678

Table 4: Impulsive conditions

P_o	I_o	
	0.250	0.500
5.361	93	187
8.587	58	116
15.312	33	65
20.000	25	50

4.4   MESH CONVERGENCE STUDY

In authors' previous work (Lee *et al*. 2015), a mesh convergence study was performed for six types of mesh sizes under a sloshing load. As a result, the element sizes for the SPB tank and the hull structure were determined as 100 and 400 mm, respectively. For this study, the number of elements generated and applied is approximately 3.4 million as shown in Figure. 10.

5.   NUMERICAL RESULTS

According to the author's previous paper (Lee *et al*. 2015), it was found that the location of Scenario-19 (Figure. 4) was the weakest structural component in the SPB tank. Thus, the parametric studies to derive the P-I diagram is performed only for this location.

5.1   PARAMETRIC STUDIES

To derive the P-I diagram of the FLNG CCS, the peak pressure and the ideal duration time from the actual sloshing loads are selected as input parameters. 30 case series analyses are performed. The parameters considered in this part of the process are as follows:

- P_o : 0.592, 1.324, 3.225, 5.361, 8.587, 15.312 bars
- t_{dur}' : 88, 108, 124, 316, 350 ms

The calculated impulse values, according to the selected peak pressures and ideal duration times, are summarised in Table 3. Furthermore, to capture the damage level near-impulsive domain in the P-I diagram, 8 more cases of series analyses are performed. The parameters considered in this part of the analysis are as follows:

- I_o : 0.250, 0.500 bar·s
- P_o : 5.361, 8.587, 15.312, 20.000 bars

The calculated duration of time for the various impulse levels and peak pressures are presented in Table 4. The dynamic structural response characteristics of the FLNG CCS are investigated using ANSYS/LS-DYNA (2014). Maximum deformation is defined as the maximum value, and the permanent deflection is the average value of event duration.

Figure. 11 describes the deformation time histories for variations in the peak pressure and the ideal duration of pressure events. Figures. 12 and 13 illustrate the maximum and the permanent deformations of the FLNG CCS. It is observed that as the impulse and peak pressure increase, the maximum deformation increases. It is found that the level of permanent deformation is not severe when the sloshing peak pressure is under 6.0 bars. However, the damage level increases significantly when peak pressures rise to over 6 bars.

Figure. 14 reveals the sensitivity of the maximum and permanent deformation to peak pressure and impulse. It appears that the main factor for increasing the maximum and permanent deformation is the peak pressure and impulse respectively.
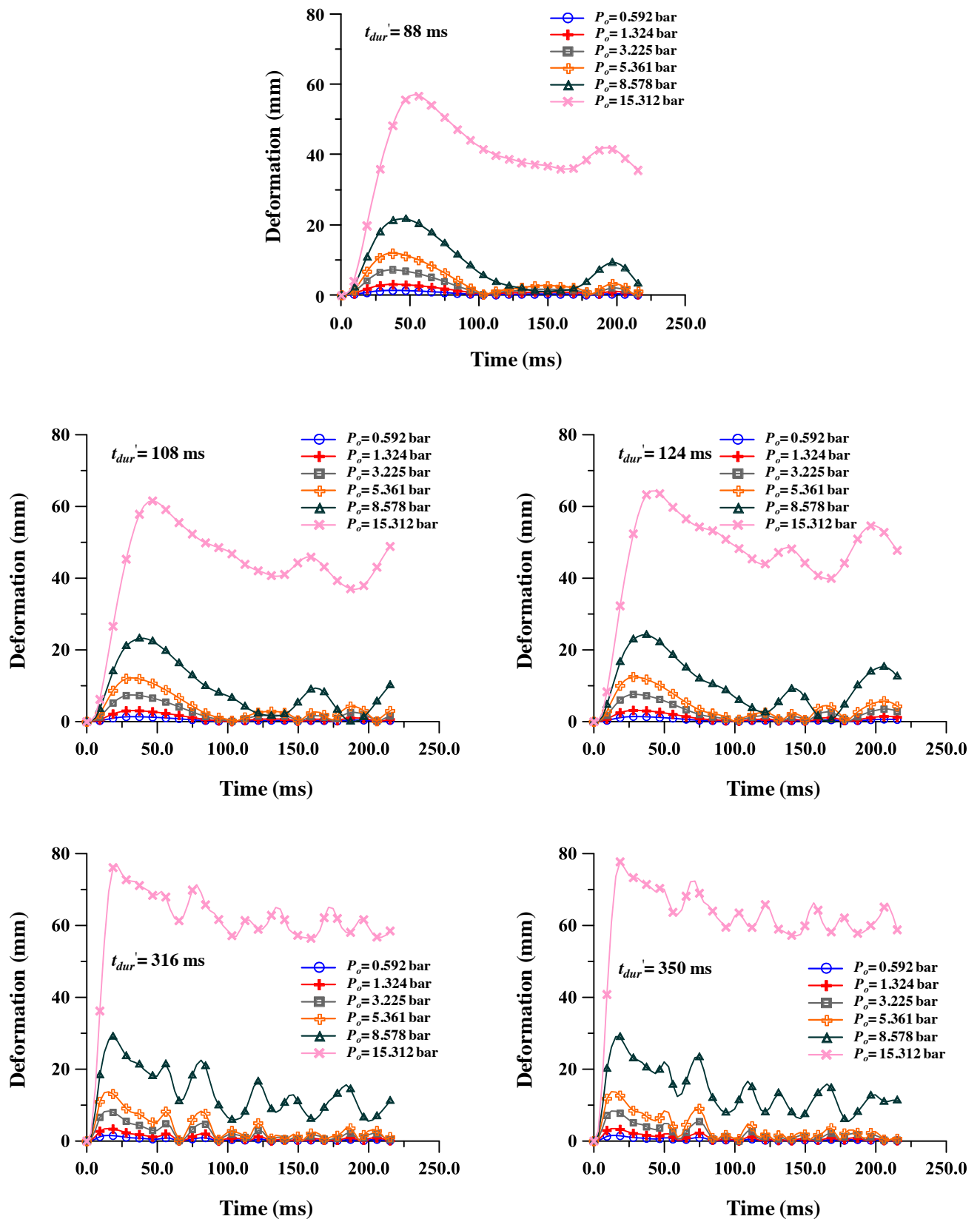
Figure 11: Deformation time-histories of the FLNG CCS under sloshing impact loads.
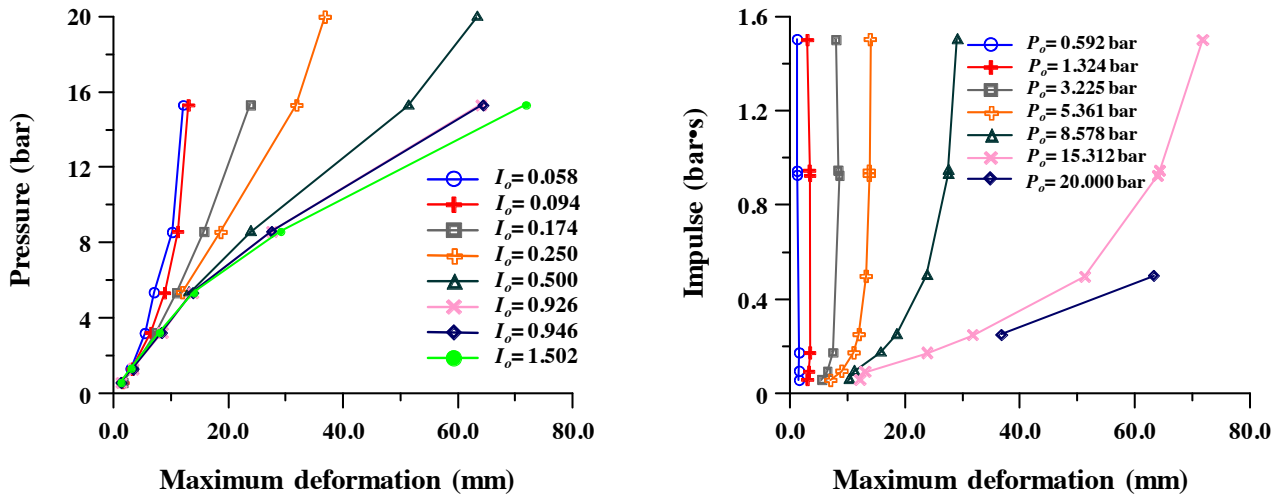
Figure 12: Maximum deformation of the FLNG CCS with varying impact load profiles.
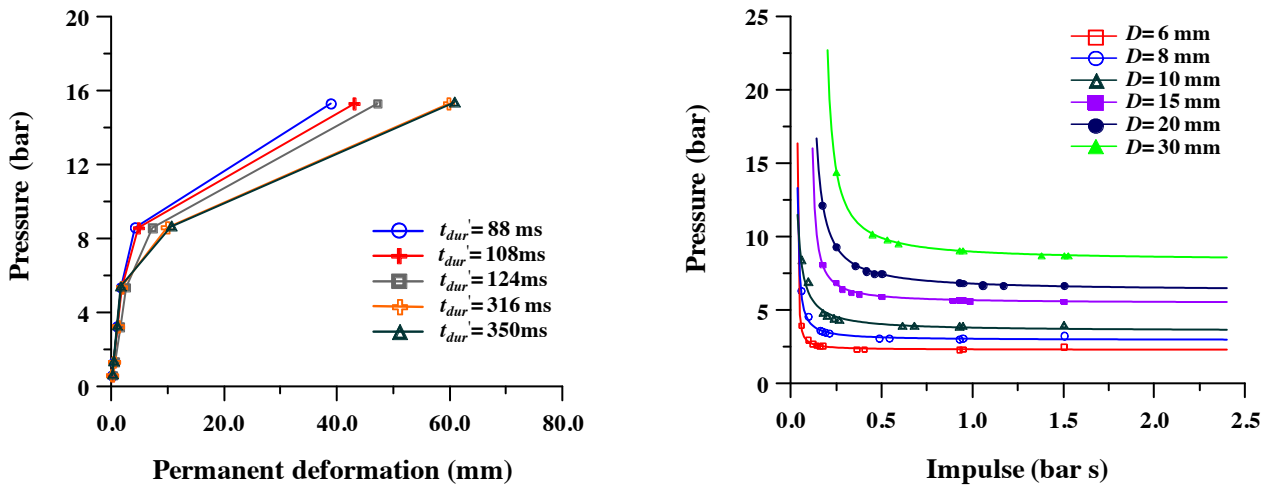

Figure 13: Permanent deformation of the FLNG CCS with varying impact load profiles.

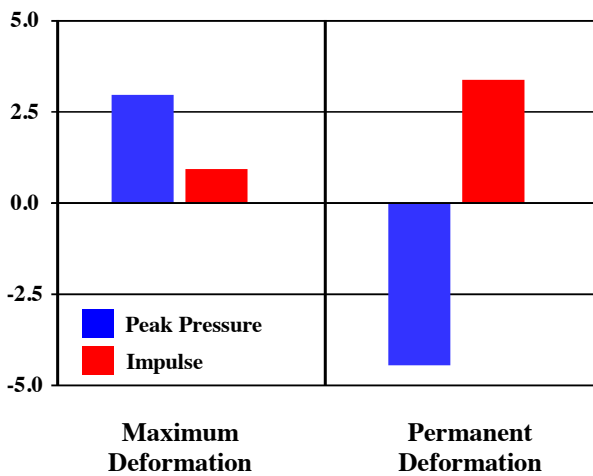Figure 15: Pressure-impulse diagram of the FLNG CCS according to the damage level.

Figure 14: Sensitivities of the peak pressure and impulse on the maximum and permanent deformation.

5.2   DERIVATION OF THE P-I DIAGRAM

To generate the P-I diagram for the FLNG CCS, a series of NLFEM analyses are conducted. The sloshing impact loads, such as the peak pressures and impulses that correspond to the LNG CCS damage levels, are plotted in the P-I space, based on the maximum deformation levels. Finally, the iso-damage curves, which are the boundary lines between different damage levels, can be obtained by using the curve fitting method.

In the present study, the simple hyperbolic function recommended by Oswald and Sherkut (1994) was used. It has been applied some engineering studies (Shi et al. 2008; Mutalib and Hao 2011) and the good results were achieved. The general form is written as follows:

$$(P - P_a)(I - I_a) = \alpha(P_a / 2 + I_a / 2)^\beta \qquad (3)$$

where P_a is the pressure asymptote for the maximum deformation level D ; I_a is the impulsive asymptote for maximum deformation level D ; and α and β are constants that determine the shape of the hyperbola which can be obtained by numerical curve fitting.

Figure. 15 illustrates the P-I diagram of the FLNG CCS. The estimated values of the asymptotes and constants are summarised in Table 5, along with the maximum deformation level.

Table 5: Approximated asymptotes and constants

D	P_a	I_a	α	β
6	2.284	0.038	0.083	-5.989
8	2.957	0.031	0.143	-1.131
10	3.516	0.010	0.464	-1.183
15	5.408	0.102	0.221	-0.135
20	6.254	0.096	0.547	-0.150
30	8.334	0.163	0.813	-0.303

6. DISCUSSION

Sloshing impact loads in cargo tanks such as LNGCs, FPSOs, FLNGs or VLCCs are among the most challenging issues for structural designers. For over the last 50 years, a number of design procedures have been proposed and applied for industrial purposes.

Apart from the industrial use of existing design procedures, the issue of how to accurately determine the sloshing scenarios and to design for sloshing loads is still controversial. To resolve this issue, the authors have introduced a novel concept, utilising a probabilistic approach to sample sloshing scenarios and to analyse the sloshing impact load profiles. Previously, the feasibility of this approach had been fully reviewed through an applied example (Paik *et al*. 2015).

In the present paper, the authors introduced a novel method to the assessment of the sloshing damage on the hypothetical FLNG tank structure and confirmed the feasibility of sloshing damage assessment. Once designers or engineers have the P-I diagram, they will be able to assess the damage level immediately. However, it is numerically very expensive to derive the P-I diagram which requires a full set of parametric simulations.

7. CONCLUSIONS

The aim of this study is to briefly introduce the developed probabilistic procedure for sloshing assessment in FLNG CCSs, and to derive a P-I diagram based on parametric studies of sloshing impact loads. The following conclusions can be drawn from the results obtained from this study.

(1) A new procedure to generate a P-I diagram of an FLNG CCS under sloshing impact loads is introduced, based on a series of NLFEM analyses. A P-I diagram of a model FLNG CCS is successfully derived, indicating the iso-damage levels.

(2) The effect of impulse and peak pressure is proportional to the maximum and permanent deformations. It was found that the peak pressure and impulse respectively play a primary role in increasing the maximum and permanent deformation.

(3) Regardless of the duration of pressure, very similar levels of permanent deformation appear when the peak pressure is under 6.0 bars.

(4) The probabilistic approach to assessing sloshing impact damage is fully presented. It includes a full series of steps, from selecting credible scenarios of tank sloshing to deriving the P-I diagram of tank structures. The feasibility of the developed procedure is confirmed by testing an applied example of a hypothetical FLNG.

It is believed and hoped that the probabilistic procedure developed in this study will be helpful for engineers and designers in the shipbuilding and offshore industries. The authors will continue their research on sloshing-induced impact loads and design loads, as there is a need to further refine the industry standards for resolving these issues. It is noted that to improve the accuracy of the proposed procedure, the effects of insulation systems and of thermal loads in the cargo tanks should be considered.

8. ACKNOWLEDGEMENTS

9. REFERENCES

1. ABS (2006) *Guidance Note on Strength Assessment of Membrane-Type LNG Containment Systems Under Sloshing Loads*. American Bureau of Shipping, Houston, TX, US.

2. ANSYS/LS-DYNA, (2014) *User's manual* (version 15.0). ANSYS Inc., Pennsylvania, US, 2014.

3. BAKER, W.E. COX, P.A. WESTINE, P.S. KULESZ, J.J. and STREHLOW, R.A. (1983)

Explosion Hazards and Evaluation. Elsevier Scientific Pub. Co., New York, US.

4. BRIZZOLARA, S., SAVIO, L., VIVIANI, M., CHEN, Y., TEMAREL, P. and COUTY, N. (2011). *Comparison of Experimental and Numerical Sloshing Loads in Partially Filled Tanks*. *Ships and Offshore Structures*, Vol. 6(1-2), pp. 15-43.

5. BV (2011) *Strength Assessment of LNG Membrane Tanks under Sloshing Loads - Guidance Note NI 564 DTR00 E*. Bureau Veritas, Paris, France.

6. DNV GL (2006) *Sloshing Analysis of LNG Membrane Tanks*, DNV classification notes no.30.9. Det Norske Veritas, Oslo, Norway.

7. FALLAH, A.S. and LOUCA, L.A. (2007) *Pressure–Impulse Diagrams for Elastic–Plastic Hardening and Softening Single-Degree-of-Freedom Models subjected to Blast Loading*. International Journal of Impact Engineering, Vol. 34, pp. 823-842.

8. GRACZYK, M. MOAN, M.K. and WU, M.K. (2007) *Extreme Sloshing and Whipping-Induced Pressures and Structural Response in Membrane LNG Tanks*. Ships Offshore Structures, Vol. 2(3), pp. 201–216.

9. GRACZYK, M. and MOAN, T. (2008) *A Probabilistic Assessment of Design Sloshing Pressure Time Histories in LNG Tanks*. Ocean Engineering, Vol. 35(8-9), pp. 834–855.

10. HIRDARIS, S.E., WHITE, N.J., ANGOSHTARI, N., JOHNSON, M.C., LEE, Y. and BAKKERS, N. (2010). *Wave Loads and Flexible Fluid-Structure Interactions: Current Developments and Future Directions*. Ships and Offshore Structures, Vol. 5(4), pp. 307-325

11. HWANG, J.O. CHUN, S.E. JOH, K.H. SAMBOS, P. DE LAUZON, J. WHITE, N. KIM, M.S. PARK, J.B. and LEE, J.M. (2014) *Direct Assessment of Structural Capacity Against Sloshing Using Dynamic Nonlinear FE Analysis*. The 24h International Offshore and Polar Engineering Conference, ISOPE, Busan, Korea, June 15–20.

12. ITO, H. SUH, Y.S. CHUN, S.E., SATISH KUMAR, Y.V. HA, M.K. PARK, J.J. YU, H.C. and WANG, B. (2008) *A Direct Assessment Approach for Structural Strength Evaluation of Cargo Containment System Under Sloshing inside LNGC Tanks based on Fluid Structure Interaction*. The 27th International Conference on Offshore Mechanics and Arctic Engineering, Estoril, Portugal, June 15-20.

13. JARRETT, D.E. (1968) *Derivation of British Explosives Safety Distances*. Annals of New York Academy of Science. 152(1), pp. 18-35.

14. JONES, N. (1970) *Structural impact*. Cambridge University Press, Cambridge, UK.

15. KIM, S.Y., KIM, Y.H. and LEE, J.H. (2017). *Comparison of Sloshing-Induced Pressure in*

16. KUO, J.F. CAMPBELL, R.B. DING, Z. HOIE, S.M. RINEHART, A.J. SANDSTORM, R.E. YUNG, T.W. GREER, M.N. and DNANCZKO, M.A. (2009) *LNG tank sloshing assessment methodology: The new generation*. International Journal of Offshore and Polar Engineering, ISOPE, Vol. 19(4), pp. 241-253.

17. LAN, S.R. and CRAWFORD, J.C. (2003) *Evaluation of the Blast Resistance of Metal Deck Proofs*. Proceedings of the fifth Asia-Pacific conference on shock & impact loads on structures, Changsha, Hunan, China, November 12-14.

18. LEE, S.E., KIM, B.J. SEO, J.K. HA, Y.C. MATUSUMOTO, T. BYEON, S.H. and PAIK, J.K. (2015) *Nonlinear Impact Response Analysis of LNG FPSO Cargo Tank Structures under Sloshing Loads*. Ships and Offshore Structures.

19. LI, Q.M. and MENG, H. (2002a) *Pressure-Impulse Diagram based on Dimensional Analysis and Single-Degree-of-Freedom Model*. Journal of Engineering Mechanics, Vol. 128(1), pp. 87–92.

20. LI, Q.M. and MENG, H. (2002b) *Pulse Loading Shape Effects on Pressure-Impulse Diagram of Elastic Plastic Structures*. International Journal of Mechanical Sciences, Vol. 44, pp. 1985-1998.

21. LIU, D., TANG, W., WANG, J., XUE, H. and WANG, K. (2017). *Hybrid RANS/LES Simulation of Sloshing Flow in a Rectangular Tank with and without Baffles*. Ships and Offshore Structures, Vol. 12(8), pp. 1005-1015.

22. LR (2009) *Ship Right-Sloshing Assessment Guidance Document for Membrane Tank LNG Operations*. Lloyd's Register, London, UK.

23. MA, G.W. SSHI, H.J. and SHU, D.W. (2007) *P-I Diagram Method for Combined Failure Modes if Rigid-Plastic Beams*. International Journal of Impact Engineering, Vol. 34, pp. 1081-1094.

24. MAYS G.C. and SMITH, P.D. (1995) *Blast Effects on Buildings: Design of Buildings to Optimize Resistance to Blast Loading*. Thomas Telford Services Ltd.

25. MERRIFIELD, R. (1993) *Simplified Calculations of Blast Induced Injuries and Damage*. Report no. 37, Health and Safety Executive Specialist Inspector.

26. MUTALIB, A.A. and HAO, H. (2011) *Development of PI Diagrams for FRP Strengthened RC Columns*, Int. J. Impact Eng. Vol. 38 (5), pp. 290–304.

27. NAM, S.K. KIM, W.S. NOH, B.J. SHIN, H.C. and CHOI, I.H. (2006) *The Parametric Study on the Response of Membrane Tanks in a Mark III Type LNG Carrier Using Fully Coupled Hydro-*

Elastic Model. International Conference on Ship and Offshore Technology, ICSOT, Busan, Korea, September 14-15.

28. NASAR, T., SANNASIRAJ, S.A. and SUNDAR, V. (2008). *Sloshing Pressure Variation in a Barge Carrying Tank*. Ships and Offshore Structures, Vol. 3(3), pp. 185-203.

29. NORSOK (1999) *Actions and action effects*, Norwegian Standards.

30. OSWALD, C. and SHERKUT, D. (1994) *FACEDAP Theory Manual Version 1.2*, US Army Corps of Engineers Omaha District, Omaha. Nebraska.

31. PAIK, J.K., KIM, K.J., LEE, J.H., JUNG, B.G. and KIM, S.J. (2016). *Test Database of the Mechanical Properties of Mild, High-Tensile and Stainless Steel and Aluminium Alloy Associated with Cold Temperatures and Strain Rates*. Ships and Offshore Structures, Vol. 12(S1), pp. S230-S256.

32. PAIK, J.K. LEE, S.E. KIM, B.J. SEO, J.K. HA, Y.C. MATSUMOTO, T. and BYEON, S.H. (2015) *Toward A Probabilistic Approach to Determine Nominal Values of Tank Sloshing Loads in Structural Design of LNG FPSOs*. Journal of Offshore Mechanics and Arctic Engineering, Vol. 137(2).

33. PAIK, J.K. and SHIN, Y.S. (2006). *Structural Damage and Strength Criteria for Ship Stiffened Panels under Impact Pressure Actions Arising from Sloshing, Slamming and Green Water Loading*. Ships and Offshore Structures, Vol.1(3), pp.249-256.

34. PAIK, J.K. and THYAMBALLI, A.K. (2003) *Ultimate limit state design of steel-plated structure*. John Wiley & Sons, Chichester, UK.

35. PAIK, J.K. and THYAMBALLI, A.K. (2007). *Ship-shaped Offshore Installations: Design, Building, and Operation*. Cambridge University Press, Cambridge, UK.

36. PASTOOL, W. OSTVOLD, T.K. BYKLUM, E. and VALSGARD, S. (2005) *Sloshing Load and Response in LNG Carriers for New Designs, New Operations and New Trades*. GasTech 2005, Bilbao, Spain, March 14-17.

37. PARLIN, N.J. DAVIDS, W.G. NAGY, E. and CUMMINS, T. (2014) *Dynamic Response of Lightweight Wood-based Flexible Wall Panels to Blast and Impulse Loading*. Construction and Building Materials, Vol. 50, pp. 237-245.

38   SCHENEIDER, P. (1998) *Predicting Damage of Slender Cylindrical Steel Shells under Pressure Wave Load*. Journal of Loss Prevention in the Process Industries, Vol. 11(3), pp. 223-228.

39. SHI, Y. HAO, H. and LI, Z.H. (2008) *Numerical Derivation of Pressure-Impulse Diagrams for Prediction of RC Column Damage to Blast Loads*. International Journal of Impact Engineering, Vol. 35, pp. 1213-1227.

40. SMITH, P.D. and HETHERINGTON, J.G. (1994) *Blast and Ballistic Loading of Structures*. Butterworth Heinemann, London, UK.

41. SOHN, J.M. KIM, S.J., KIM, B.H. and PAIK, J.K. (2013) *Nonlinear Structural Consequence Analysis of FPSO Topside Blast Walls*. Ocean Engineering, Vol. 60.

42. XU, Q., HU, Z. and JIANG, Z. (2017). *Experimental Investigation of Sloshing Effect on the Hydrodynamic Responses of an FLNG System during Side-by-Side Operation*. Ships and Offshore Structures, Vol. 12(6), pp.804-817.

43. WESEVICH, J.W. and OSWARD, C.J. (2005) *Empirical based Concrete Masonry Pressure–Impulse Diagrams for Varying Degrees of Damage*. Structures Congress 2005, New York, US.

44. ZHANG, J., WU, W. and HU, J. (2017). *Parametric Studies on Nickel Ore Slurry Sloshing in a Cargo Hold by Numerical Simulations*. Ships and Offshore Structures, Vol.12(2), pp.209-218.

45. ZHAO, W., YANG, J. and HU, Z. (2013). *Effects of Sloshing on the Global Motion Responses of FLNG*. Ships and Offshore Structures, Vol. 8(2), pp.111-122.